International Journal of Chemical Sciences

Research Article | Vol 20 Iss 3

Spectroscopic Studies of 3-Furan-2-yl-4-Phenyl-Butyric Acid Compound DFT Method (FTIR and FT-Raman), NBO Analysis, Homo-Lumo, First Order Hyper polarizability and Docking Studies

P Chakkaravarthy*
Department of Chemistry, Government Thirumagal Mills College Gudiyattam, Tamil Nadu, India

***Corresponding author:** P Chakkaravarthy, Department of Chemistry, Government Thirumagal Mills College Gudiyattam, Tamil Nadu, India, Tel: 6369462485; E-mail: p.chakku766@gmail.com

Received: June 23, 2022, Manuscript No. tsijcs-22-67457; **Editor assigned:** June 27, 2022, PreQC No. tsijcs-22-67457; **Reviewed:** July 11, 2022, QC No. tsijcs-22-67457; **Revised:** August 22, 2022, Manuscript No. tsijcs-22-67457; **Published:** August 29, 2022, DOI:10.37532/0972-768X.22.20.430

Abstract

The goal of this research is to characterize 3-furan-2-yl-4-phenyl-butyric acid. The molecule was created using quantum chemistry and vibrational spectrum techniques. The ideal molecular geometry (bond length, bond angle), whole vibrational frequency, infrared intensities, and Raman scattering activities were determined using the Density Functional Theory (DFT) B3LYP approach with the 6-311++G (d, p) basis set. The estimated HOMO-LUMO band gap energies confirm charge transport within the molecule. The hyper conjugative interaction energy E (2) and the electron densities of donor I and acceptor (j) bonds were calculated using NBO analysis. Other factors were calculated and analyzed in addition to NLO and MEP. Molecular docking was performed to determine the hydrogen bond lengths and binding energy with numerous different molecules to study the investigation molecule's biological activities.

***Keywords:** Hyper conjugative interaction, Density functional theory, HOMO-LUMO band gap*

Introduction

The vibrational spectroscopic studies of anti-inflammatory molecule 3-furan-2-yl-4-phenyl-butyric acid with the help of DFT method. It is used to fever, stiffness, swelling and relieve pain. The title molecule is soluble in water and sparingly insoluble in alcohol.

An extensive literature survey conducted reveals that a great deal of research has been done on aryl propionic acids and its substituted derivatives. Structure characterization investigation of ketoprofen, a propanoic acid derivative by combined quantum chemical calculations and spectroscopic analysis was done by ML Vueba [1]. Various other properties of propionic acids and its substituted derivatives have also been studied to state its uses in biological field. Photo degradation mechanism of Non-steroidal anti-inflammatory drugs containing Thiophene moieties: Suprofen and Tiaprofenic Acid by Klefah AK Musa is one such work [2]. Molecular mobility of ibuprofen and ketoprofen was evaluated with respect to the different inter molecular linear/cyclic hydrogen bonding associations by MT Ottou Abe [3].

Quantum chemical computational techniques have proved to be an indispensable tool for deducing and predicting the vibrational spectra [4,5]. Sophisticated electron correlation and density functional theory calculations are increasingly available and deliver force field of high precision even for large polyatomic molecules [6,7]. Neither the complete spectroscopy analysis nor the quantum chemical calculations for the title compound have been reported so far on the basis of the literature survey done. The objective of the present study is to give a complete account of the molecular geometry and vibrations of the title molecule. For that purpose, quantum chemical computations were carried out to study conformational stability analysis, molecular structure and FT-IR spectral investigation of 3-furan-2-yl-4-phenyl-butyric acid using Density Functional Theory (DFT). Vibrational spectra have been analyzed on the basis of calculated Potential Energy Distribution (PED). Mean polarizability, dipole moment and first order hyperpolarisability have been investigated by ad initio DFT methods. In addition to this, ab initio and density

Citation: P Chakkaravarthy. Spectroscopic Studies of 3-Furan-2-yl-4-Phenyl-Butyric Acid Compound DFT Method (FTIR and FT-Raman), NBO Analysis, Homo-Lumo, First Order Hyper polarizability and Docking Studies. Int J Chem Sci. 2022;20(3):430

functional theory calculations using 6-311++G (d, p) basis set were used to determine the HOMO-LUMO energy.

Materials and Methods

Experimental details

The title compound in the solid state was procured from Sigma Aldrich chemical company with a stated purity 98% and it was used without further purification. The FT-IR spectrum was recorded in the region 4000–450 cm^{-1} with the sample in the KBr pellet, using Perkin Elmer FT-IR spectrometer. The resolution of the spectrum is 4 cm^{-1}. The FT-Raman spectrum was obtained in the range 4000–100 cm^{-1} using Bruker RFS 100/S FT-Raman spectrophotometer with a 1064 nm Nd: YAG laser source of 100 mW power. All the experimental spectral data (FT-IR, FT-Raman) collected from SAIF, IIT, Chennai, India.

Computational details

The spectroscopic analysis and the quantum chemical calculations which comprises of the optimized structure of the title compound, corresponding energy and vibrational harmonic frequencies were calculated by using DFT (B3LYP) with 6-311++G (d,p) basis set using GAUSSIAN 03W program package [8]. 6-311++G is a split-valence triple-zeta basis and adds one Gaussian Type Orbitals (GTO) to 6-31G that uses three sets of contracted functions for each valence orbital type [9,10]. The geometric structure as well as parameters, namely bond angle and bond length were obtained from CHEMCRAFT software.

Vibrational frequencies are scaled 0.9461 for B3LYP/6-311++G (d,p). The symmetry considerations and the vibrational assignments are made with a high degree of accuracy using the Vibrational Energy Distribution Analysis (VEDA) software [11]. The GABEDIT software and ORIGIN6.1 software were used to generate the theoretical and experimental IR and RAMAN spectrum and the spectra were compared. The hyperpolarisability for the title molecule was also calculated at B3LYP level using the basis set 6-311++G (d,p) Polar = enonly. By using the Gaussian 03W output the thermodynamical variables were found out using THERMO.PL [12]. The correlation graphs of the thermodynamical variables (entropy, enthalpy and heat capacity) *vs.* temperature were plotted for the title compound. The Molecular Electrostatic Potential (MEP) was also calculated using Gauss View. The Natural Bond Orbital (NBO) was calculated of the title molecule at B3LYP level using the basis set 6-311++ G (d,p) POP=NBO test. This analysis is done to give clear evidence of stabilization originating from hyper conjugation of various intra molecular interactions [13-15]. The Raman activities (S_i), calculated with the GAUSSIAN 03W program, were subsequently converted to relative Raman intensities (I_i) using the following relationship derived from the theory of Raman scattering using raint program [16,17].

$$I_i = \frac{f(\upsilon_0-\upsilon_i)^4 S_i}{\upsilon_i [1 - \exp (hc\upsilon i/k_b T)]}$$

Where υ_0 is the laser excitation frequency in cm^{-1} (in this work, the excitation wave number, υ_0=9398.5 cm^{-1}, which corresponds to the wavelength of 1064 nm of a Nd: YAG laser, υ_i is the vibrational wavenumber of the i^{th}normal mode in cm^{-1}, h, k_bc and T are the fundamental constants Planck constant, Boltzmann constant, speed of light and temperature in Kelvin, respectively.

Results and Discussion

Geometrical structure

The optimized structure parameters of the title compound were calculated at B3LYP levels and are recorded in (Table 1). In accordance with the atom numbering scheme as obtained from CHEMCRAFT software and represented in (Figure 1). This molecule has fourteen C-C bond lengths, four C-O bond lengths, thirteen C-H bond lengths and one O-H bond length. The molecular geometry in the gas phase may differ from the solid phase, owing to the extended hydrogen bonding and staking interactions. From theoretical values, any variation in the optimized bond lengths is because the theoretical values belong to the isolated molecules in gas phase and the experimental values belong to the molecules in solid state [18]. It is observed that the calculated C-C bond lengths and the O-C bond lengths are found to be nearly identical at all calculation levels. The average value of the bond distances of C-C and C-H in the benzene ring calculated by density functional theory method with same basis sets are 1.529 A and 1.098 A, respectively. Inclusion of OH and CH atoms brings a strong electron withdrawing nature to the

compound and thus is expected to contribute to the formation of a resonance structure. This is the reason for the shortening of bond lengths O_2-H_{31}=0.981 Å and C_9-H_{23}=1.08 Å obtained by DFT method compared to other bond lengths like C_4-C_5=1.535 Å. In this title molecule the bond angle C_7-O_1-C_{14}= 104.3^o is smaller than the other bond angle C_{16}-C_{17}-H_{30}=120^o calculated.

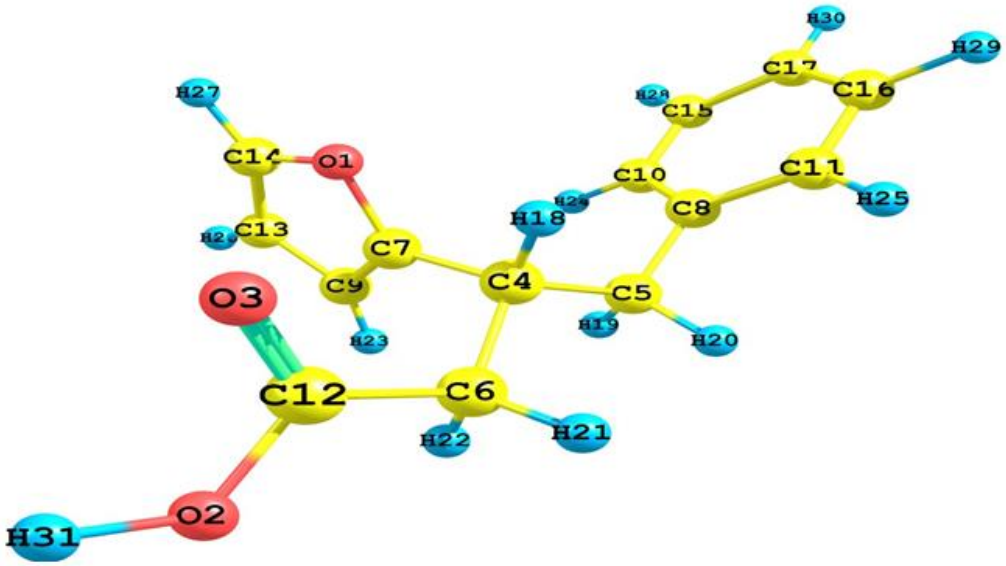

FIG.1**. Optimized geometric structure with atom numbering of 3-Furan-2-yl-4-Phenyl-Butyric Acid (2F4PBA).**

TABLE 1. **Optimized geometrical parameters of 3-Furan-2-yl-4-Phenyl-Butyric Acid (2F4PBA).**

Parameter bond length (Å)	**B3LYP/ 6-311++ G(d,p)**	**Parameter bond angle (0)**	**B3LYP/ 6-311++ G(d,p)**
O_1-C_7	1.333	C_7-O_1-C_{14}	104.3
O_1-C_{14}	1.359	O_1-C_7-C_4	114
O_2-C_{12}	1.358	O_1-C_7-C_9	114.7
O_2-H_{31}	0.981	O_1-C_{14}-C_{13}	110.6
O_3-C_{12}	1.222	O_1-C_{14}-H_{27}	115.6
C_4-C_5	1.549	C_{12}-O_2-H_{31}	111.9
C_4-C_6	1.544	O_2-C_{12}-C_3	123.7
C_4-C_7	1.529	O_2-C_{12}-C_6	110
C_4-H_{18}	1.1	O_3-C_{12}-C_6	126.3
C_5-C_8	1.511	C_5-C_4-C_6	111.1
C_5-H_{19}	1.098	C_5-C_4-C_7	111.6
C_5-H_{20}	1.099	C_5-C_4-H_{18}	108.4
C_6-C_{12}	1.512	C_4-C_5-C_8	113.3
C_6-H_{21}	1.096	C_4-C_5-H_{19}	111.2
C_6-H_{22}	1.097	C_4-C_5-H_{20}	109.4
C_7-C_9	1.336	C_6-C_4-C_7	110.6
C_8-C_{10}	1.385	C_6-C_4-C_{18}	107.2
C_8-C_{11}	1.385	C_4-C_6-C_{12}	113.1

C_9-C_{13}	1.415	C_4-C_6-C_{21}	110.3
C_9-H_{23}	1.08	C_4-C_6-H_{22}	109.5
C_{10}-C_{15}	1.395	C_7-C_4-H_{18}	107.7
C_{10}-H_{24}	1.086	C_4-C_7-C_9	131.3
C_{11}-C_{16}	1.395	C_8-C_5-H_{19}	109.7
C_{11}-H_{25}	1.086	C_8-C_5-H_{20}	107.7
C_{13}-C_{14}	1.375	C_5-C_8-C_{10}	119.3
C_{13}-H_{26}	1.08	C_5-C_8-C_{11}	119.3
C_{14}-H_{27}	1.08	H_{19}-C_5-H_{20}	105
C_{15}-C_{17}	1.395	C_{12}-C_6-H_{20}	107.1
C_{15}-H_{28}	1.086	C_{12}-C_6-H_{22}	108.9
C_{16}-C_{17}	1.395	H_{21}-C_6-H_{22}	107.8
C_{16}-H_{29}	1.086	C_7-C_9-C_{13}	104.3
C_{17}-H_{30}	1.086	C_7-C_9-H_{23}	128.3
		C_{10}-C_8-C_{11}	121.4
		C_8-C_{10}-C_{15}	119.3
		C_8-C_{10}-H_{24}	121.4
		C_8-C_{11}-C_{16}	119.3
		C_8-C_{11}-H_{25}	121.3
		C_{13}-C_9-H_{23}	127.5
		C_9-C_{13}-C_{14}	106.1
		C_9-C_{13}-H_{26}	127.6
		C_{15}-C_{10}-H_{24}	119.3
		C_{10}-C_{15}-C_{17}	120
		C_{10}-C_{15}-H_{28}	120
		C_{16}-C_{11}-H_{25}	119.5
		C_{11}-C_{16}-C_{17}	120
		C_{11}-C_{16}-H_{29}	120
		C_{14}-C_{13}-H_{26}	126.3
		C_{13}-C_{14}-H_{27}	133.8
		C_{17}-C_{15}-H_{28}	120
		C_{15}-C_{17}-C_{16}	120
		C_{15}-C_{17}-H_{30}	120
		C_{17}-C_{16}-H_{29}	120
		C_{16}-C_{17}-H_{30}	120

Donor acceptor interactions

In quantum chemistry, a calculated bonding orbital with maximum electron density forms a natural bond orbital or NBO. In computational chemistry the localized orbitals are used to calculate the distribution of electron density in atoms and in bonds between atoms. The details obtained about the interactions in both filled and virtual orbital space can complement the study of both inter and intra molecular interactions, which is the basis of studying NBO. That is why NBO analysis is proved to be an important tool for chemical analysis of hyper conjugative interaction and electron density transfer from filled lone electron pairs of the Lewis base (an electron pair donor) Y into the unfilled anti bond σ^* (X-H) of the Lewis acid (an electron pair acceptor) X-

H in X-Y….Y hydrogen bonding systems [19]. The magnitude of energy of hyper conjugative interactions, E (2) forms the basis of studying the strength of the interaction between electron donors and electron acceptors, or the donating affinity from electron donors to acceptors and hence the degree of conjugation of the entire system. The second-order Fock matrix was done to evaluate the donor–acceptor interactions in NBO analysis [20]. The interactions cause loss of occupancy from the localized natural bond orbitals of the idealized Lewis structure into an empty non-Lewis orbital. For each donor (i) and acceptor (j), the stabilization energy E (2) related with the delocalization i → j is estimated as

$$E\ (2) = \Delta E_{ij} = q_i\ (F_{ij})^{2} / (\varepsilon_j - \varepsilon_i)$$

Where q_i is the donor orbital occupancy
ε_j and ε_i are diagonal elements
F_{ij} is the off diagonal NBO Fock matrix element.

Delocalization of electron density between occupied Lewis type (lone or bond pair) natural bonding orbitals and previously unoccupied non Lewis (anti bond or Rydberg) natural bonding orbitals correspond to a stabilizing donor–acceptor interaction. In order to interpret the intermolecular hydrogen bonding, Intermolecular Charge Transfer (ICT) and delocalization of electron density, NBO analysis was performed on the title molecule using B3LYP/6-311++G (d,p) Pop=NBO test basis set and the corresponding results are presented in Table 2. Intensity of the interaction between electron donors and electron acceptors is directly dependent on E (2) value, *i.e.* more the donating tendency from electron donors to electron acceptors, greater is the extent of conjugation of the whole system. The intra-molecular interaction is formed by the orbital overlap between σ(C-C) and σ^*(C-C) bond orbital which results in Intra-molecular Charge Transfer (ICT) causing stabilization of the system. These interactions are observed as increase in Electron Density (ED) in C-C, C-H, C-O and O-H anti-bonding orbital that weakens the respective bonds. NBO analysis was performed on the molecule at the DFT/B3LYP6-31++G (d,p) level in order to explicate the delocalization of electron density within the molecule. The delocalization of σ electron from σ (C_1-C_2) distribute to anti-bonding σ^* (C_2-C_3), σ * (C3-C14), σ^* (O_6-H_{23}) leading to the stabilization energy of 0.84 kJ/mol, 1.99 kJ/mol, 2.95 kJ/mol, respectively due to conjugative interactions.

A strong interaction has been observed due to the electron density transfer from the Lone Pair (LP) (1) of Oxygen atom (O_5) to anti-bonding orbital σ^*(C_1-C_6) with a large stabilization energy of 32.76 kJ/mol. In the case of LP (1) of Oxygen atom (O_{13}) to the anti-bonding acceptor σ^*(C_{14}-C_{15}) and σ^*(C_{16}-C_{17}) has low stabilization energy of 5.82 kJ/mol and 6.67 kJ/mol respectively as shown in Table 2. The interaction energy, related to resonance in the molecule, is electron withdrawing from the ring through π^* (C_{16}-C_{17}) of the NBO conjugated with π^*(C_{14}-C_{15}) resulting with large stabilization energy of 86.64 kJ/mol. Similarly, π^*(C_{16}-C_{17}) of the NBO conjugated with π^*(C_{14}-C_{15}) resulting with l stabilization energy of 22.916 kJ/mol. Therefore, the maximum energy delocalization takes place in the π^*-π^* transition (Table 2).

TABLE 2. **Second order perturbation theory analysis of Fock matrix in NBO basis of 3-Furan-2-yl-4-Phenyl-Butyric Acid (2F4PBA).**

Donor	Type	ED/e (qi)	Acceptor	Type	ED/e (qi)	E(2) kcal/mol	E(j)-E(i) a.u.	F(i,j) a.u.
C_1-C_2	σ	1.97649	C_2-C_3	σ^*	0.02832	0.84	1.05	0.026
C_1-C_2	σ		C_3-C_{14}	σ^*	0.03625	1.99	1.09	0.042
C_1-C_2	σ		O_6-H_{23}	σ^*	0.01301	2.95	1.01	0.049
C_1-O_5	σ	1.99594	C_1-C_2	σ^*	0.05163	1.39	1.46	0.041
C_1-O_5	π		C_2-H_{18}	σ^*	0.01321	1.12	0.76	0.026
C_1-O_5	π		C_2-H_{19}	σ^*	0.01189	1.16	0.76	0.027
C_2-C_3	σ	1.96944	O_{13}-C_{14}	σ^*	0.03051	2.02	1.16	0.043
C_2-C_3	σ		C_{14}-C_{15}	π^*	0.01736	1.77	0.66	0.033
C_2-H_{18}	σ	1.96451	C_1-O_5	π^*	0.20558	4.22	0.52	0.044
C_2-H_{19}	σ	1.96637	C_1-O_5	π^*	0.20558	4.43	0.51	0.045
C_2-H_{19}	σ		C_3-C_4	σ^*	0.02044	3.06	0.9	0.047
C_7-C_8	σ	1.96563	C_{12}-H_{28}	σ^*	0.0316	3.28	1.18	0.056

C_7-C_{12}	σ	1.96321	C_4-C_7	σ^*	0.0282	3.23	1.17	0.055
C_7-C_{12}	σ		C_7-C_8	σ^*	0.02832	6.29	1.4	0.084
C_7-C_{12}	σ		C_8-H_{24}	σ^*	0.02054	3.1	1.13	0.053
C_7-C_{12}	σ		C_{11}-C_{12}	σ^*	0.022	6.08	1.4	0.083
C_7-C_{12}	π	1.64556	C_8-C_9	π^*	0.33302	21.44	0.31	0.073
C_7-C_{12}	π		C_{10}-C_{11}	π^*	0.33941	23.91	0.31	0.077
C_8-C_9	σ	1.97189	C_4-C_7	σ^*	0.0282	4.64	1.17	0.066
C_8-C_9	σ		C_7-C_8	σ^*	0.02832	5.9	1.4	0.081
C_8-C_9	σ		C_{10}-H_{26}	σ^*	0.02832	2.95	1.14	0.052
C_8-C_9	π	1.67124	C_7-C_{12}	π^*	0.34503	24.26	0.32	0.079
C_8-C_9	π		C_{10}-C_{11}	π^*	0.33941	21.68	0.31	0.074
C_8-H_{24}	σ	1.97602	C_7-C_8	σ^*	0.02832	1.56	1.18	0.038
C_8-H_{24}	σ		C_7-C_{12}	σ^*	0.03116	5.4	1.18	0.071
C_9-C_{10}	σ	1.97315	C_8-C_9	σ^*	0.02002	4.62	1.4	0.072
C_9-C_{10}	σ		C_8-H_{24}	σ^*	0.02054	3.15	1.14	0.054
C_{10}-C_{11}	σ	1.97239	C_{12}-H_{28}	σ^*	0.0316	3.27	1.18	0.056
C_{10}-C_{11}	π		C_7-C_{12}	π^*	0.34503	20.49	0.32	0.073
C_{10}-C_{11}	π	1.66997	C_8-C_9	π^*	0.33302	23	0.31	0.076
C_{10}-H_{26}	σ	1.9762	C_8-C_9	σ^*	0.02002	4.19	1.17	0.063
C_{10}-C_{11}	σ	1.97239	C_{11}-C_{12}	σ^*	0.022	4.97	1.41	0.075
C_{10}-C_{11}	σ		C_9-C_{10}	σ^*	0.02062	4.59	1.4	0.072
C_{12}-H_{28}	σ	1.95559	C_3-H_{20}	σ^*	0.04076	8.72	0.92	0.08
C_{12}-H_{28}	σ		C_7-C_8	σ^*	0.02832	4.91	1.19	0.068
C_{12}-H_{28}	σ		C_7-C_{12}	σ^*	0.03116	1.87	1.19	0.042
C_{12}-H_{28}	σ		C_{10}-C_{11}	σ^*	0.02103	3.69	1.18	0.059
C_{14}-C_{15}	π	1.8358	C_{16}-C_{17}	π^*	0.32956	16.98	0.29	0.065
C_{16}-C_{17}	σ	1.97174	C_{15}-H_{29}	σ^*	0.02248	10.24	1.1	0.095
C_{16}-C_{17}	π	1.83396	C_{14}-C_{15}	π^*	0.34609	22.91	0.31	0.078
O_5	LP(2)	1.86237	C_1-C_2	σ^*	0.05163	15.76	0.64	0.092
O_5	LP(2)		C_1-O_6	σ^*	0.09678	32.76	0.63	0.129
O_6	LP(2)	1.82122	C_1-O_5	π^*	0.20558	44.87	0.36	0.114
O_{13}	LP(1)	1.94807	C_{14}-C_{15}	σ^*	0.02885	5.82	1.21	0.076
O_{13}	LP(1)		C_{16}-C_{17}	σ^*	0.02036	6.67	1.12	0.078
O_{13}	LP(1)		C_{17}-H_{31}	σ^*	0.02787	4.12	0.96	0.056
O_{13}	LP(2)	1.63051	C_{14}-C_{15}	π^*	0.34609	44.54	0.41	0.122
O_{13}	LP(2)		C_{16}-C_{17}	π^*	0.32956	44.03	0.39	0.118
C_7-C_{12}	π^*	0.34503	C_4-H_{22}	σ^*	0.01576	1.47	0.32	0.046
C_{14}-C_{15}	π^*	0.34609	C_2-C_3	σ^*	0.02123	1.56	0.34	0.048
C_{14}-C_{15}	π^*		C_3-C_4	σ^*	0.02044	1.51	0.35	0.048
C_{16}-C_{17}	π^*	0.32956	C_{14}-C_{15}	π^*	0.34609	86.64	0.03	0.073

Vibrational spectral analysis

The title molecule consists of 31 atoms, so it has 3N-6 *i.e*. 87 modes of vibration. The Vibrational frequencies are scaled 0.9642 for B3LYP/6-311++G (d,p) in order to compensate for the errors arising from the basis set incompleteness and neglect the vibrational anharmonicity. The vibrational assignments were made using the VEDA software. For the IR and Raman spectrum

plots Lorentzian band is used. Figure 2 and 3 shows comparative representations of theoretically spectra at B3LYP level of theory along with experimental spectra. The calculated wavenumber, Raman activities, IR intensities are represented in Table 3. Plotting a correlation graph between the scaled frequency and the IR and Raman frequencies represented in Figure 4 shows a corresponding fitting factor of 0.9987 and 0.9998 respectively (Table 3).

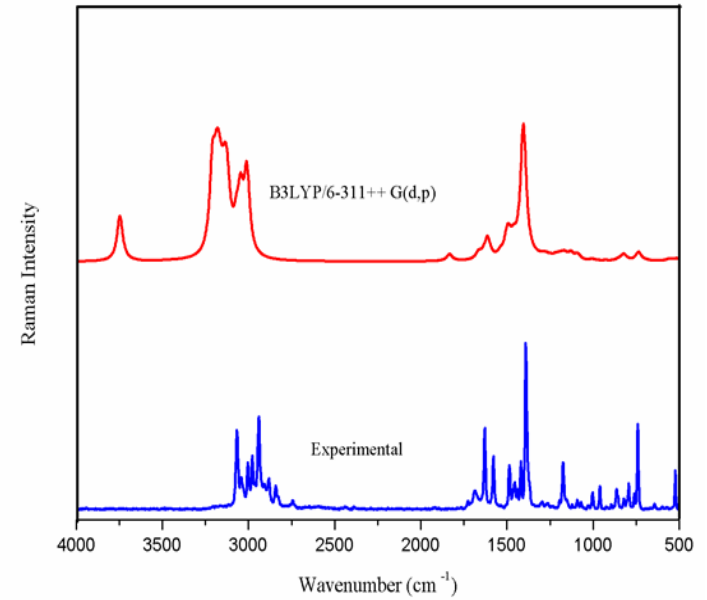

FIG. 2. **FT-Raman spectra of (+)-(S)-2-(6-methoxynaphthalen-2-yl) propanoic acid using DFT/6-311++G (d,p) and experimental data.**

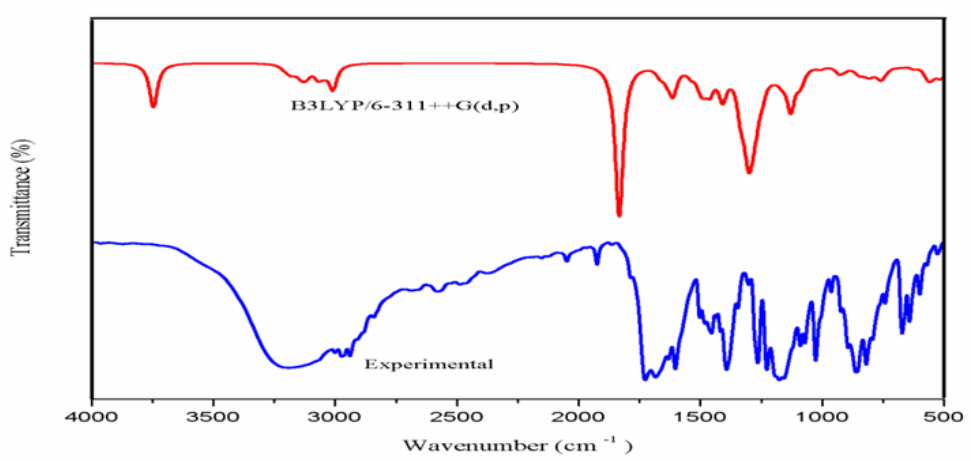

FIG.3. **FT-IR spectra of 3-furan-2-yl-4-phenyl-butyric acid using DFT/6-311++G (d,p) and experimental data**.

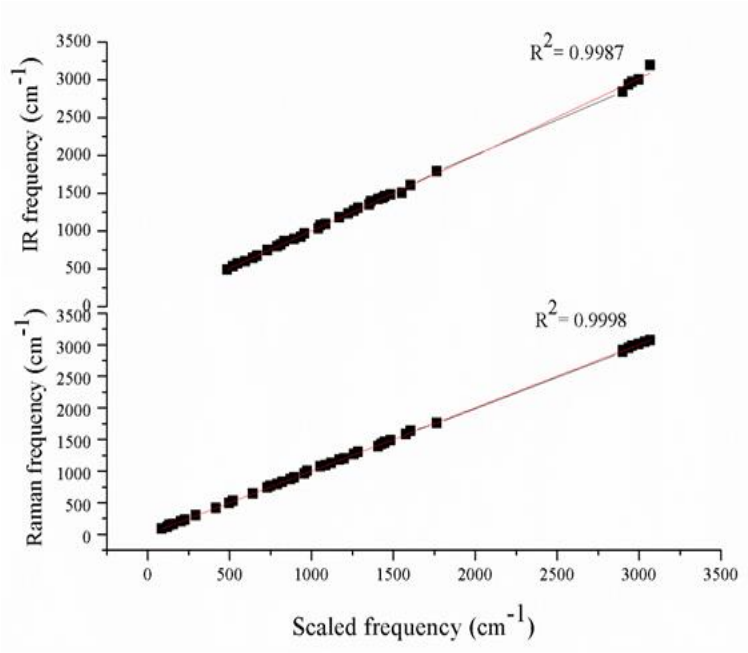

FIG.4. **Correlation graph representing scaled, IR and Raman frequencies of 3-furan-2-yl-4-phenyl-butyric acid.**

TABLE 3**. Observed and calculated vibrational frequency of 3-furan-2-yl-4-phenyl-butyric acid.at B3LYP method with 6-311++G(d,p) basis set.**

Sl. No	Frequency (cm^{-1})				Intensity				[d]Assignments (PED ≥ 10%)
	Experimental		Theoretical		IR		Raman		
	FT-IR	FT-Raman	Unscaled	[a]Scaled	[b]Relative	Absolute	[c]Relative	Absolute	
1	-	-	3753	3607	73	19	141	42	υOH (100)
2	-	-	3299	3170	0	0	202	60	υCH (90)
3	-	-	3276	3148	1	0	46	14	υCH (89)
4	3192 (vvw)	3068 (m)	3261	3134	5	1	177	53	υCH (53)
5	-	-	3205	3080	17	5	70	21	υCH (95)
6	-	-	3193	3069	32	8	61	18	υCH (96)
7	-	3042 (vw)	3185	3061	7	2	62	19	υCH (98)
8	-	-	3173	3049	3	1	109	33	υCH (90)
9	-	-	3171	3047	11	3	142	43	υCH (73)
10	3000 (vw)	3004 (w)	3131	3009	6	2	35	10	υCH (97)
11	2973 (vw)	2978 (w)	3081	2961	17	4	70	21	υCH (50)
12	2938 (vw)	2940 (m)	3067	2947	2	1	161	48	υCH (58)
13	-	2908 (vw)	3063	2944	6	1	88	26	υCH (87)
14	2843 (m)	2884 (vw)	3036	2918	23	6	161	48	υCH (93)
15	1786 (s)	1726 (vw)	1813	1742	381	100	21	6	υOC (60)

16	1603 (vvw)	1629 (m)	1654	1589	7	2	21	6	υOC (11)+υCC (34)
17	-	1579 (w)	1634	1570	4	1	10	3	υCC(55)
18	1503 (m)	-	1632	1568	0	0	64	19	υCC(26)+βCCC(14)
19	1481 (m)	1487 (w)	1541	1481	16	4	14	4	υCC(28)+βHCC(13)
20	1454 (w)	1455 (vw)	1533	1474	11	3	5	2	βHCH(60)
21	-	1438 (vw)	1492	1434	10	3	36	11	βHCH(15)
22	-	-	1485	1427	1	0	15	4	βHCH(70)+τHCCC(11)
23	-	-	1474	1417	12	3	15	5	βHCH(34)+τHCOC(14)
24	1435 (m)	-	1427	1372	1	0	5	2	βHCC(11)+βHCH(43)
25	-	1419 (w)	1386	1332	11	3	12	4	β HCH(53)
26	1417 (m)	1391 (vs)	1377	1323	7	2	42	13	υCC(20)+βHCC(28)
27	1393 (vvw)	-	1360	1307	1	0	3	1	βHCH(28)
28	-	-	1356	1303	42	11	82	24	υCC(24)+βCCC(10)
29	1346 (m)	-	1344	1292	16	4	334	100	υCC(10)+βHCC(10)+βHCH(13)
30	-	-	1339	1286	5	1	3	1	υCC(33)+βHCC(18)
31	1302 (s)	1295 (vw)	1294	1244	3	1	4	1	βHCC(34)+τHCCO(22)
32	1264 (w)	1266 (vw)	1266	1217	2	1	4	1	βHOC(12)+τHCCO(19)
33	-	-	1245	1197	26	7	4	1	βHOC(12)+βHCC(31)
34	-	-	1224	1177	6	1	4	1	υCC(10)
35	1227 (vw)	-	1212	1165	45	12	8	2	βHOC(17)
36	-	1195 (vw)	1207	1160	3	1	7	2	υCC(40)
37	1175 (vvw)	1174 (w)	1194	1147	17	4	10	3	βHCC(17)+τHCOC(30)
38	-	-	1184	1138	0	0	4	1	υCC(12)+βHCC(11)+τHCOC(23)
39	-	-	1165	1119	1	0	7	2	βHCC(64)
40	-	-	1150	1106	146	38	4	1	υOC(12)+υCC(12)+βHCC(21)
41	-	-	1113	1070	5	1	2	1	βHCH(14)+τHCOC(67)
42	-	1121 (vw)	1100	1057	3	1	15	4	υCC(30)+βHOC(20)

43	1089 (w)	1092 (vw)	1071	1029	10	3	20	6	βCCC(13)
44	1071 (w)	1071 (vw)	1053	1012	4	1	1	0	υCC(14)
45	-	-	1038	997	38	10	15	4	υCC(32)
46	1027 (w)	-	1030	990	7	2	3	1	υOC(11)+τHCCC(21)
47	-	1004 (w)	1015	975	0	0	2	1	υOC(40)+βCCC(25)
48	-	-	1001	962	0	0	3	1	υCC(22)+τHCCO(10)+τHCCC(14)
49	963 (s)	961 (w)	989	951	15	4	1	0	τHCCC(57)
50	923 (m)	-	981	943	0	0	1	0	τHCCC(31)
51	894 (w)	895 (w)	934	898	7	2	2	1	βCCC(27)
52	-	865 (vw)	916	880	3	1	1	0	βCCC(52)+τCCCC(10)
53	859 (vw)	-	900	865	6	2	1	0	τHCCC(22)
54	-	821 (vw)	891	856	6	2	2	1	τHCCC(76)
55	819 (vw)	-	883	849	9	2	3	1	βCCC(34)
56	793 (w)	793 (w)	872	838	0	0	20	6	τHCCC(21)+ωOCOC(23)
57	-	-	857	824	0	0	0	0	τCCCC(27)
58	-	761 (vw)	820	788	2	0	1	0	τHCCC(55)
59	741 (s)	741 (m)	810	778	19	5	0	0	υCC(11)
60	-	-	758	728	40	10	27	8	βCCC(32)
61	672 (m)	-	739	710	68	18	2	1	υOC(12)+βOCO(26)
62	641 (m)	643 (vw)	732	703	27	7	1	0	τHCCC(11)+τCCCC(25)+ωCCCC(15)
63	-	-	710	682	28	7	2	1	βCCC(10)+βOCO(22)+βCOC(10)
64	599 (s)	-	696	669	13	3	1	0	βCCC(37)+ωCCCC(18)
65	570 (vs)	-	657	631	58	15	3	1	τHOCC(74)
66	-	-	634	610	0	0	4	1	βOCO(13)+βCCC(15)
67	527 (vs)	523 (w)	610	586	17	5	1	0	τCCCC(15)+ωCCCC(14)
68	-	493 (vw)	607	584	7	2	5	2	βHCC(13)
69	483 (m)	-	600	576	35	9	2	1	βCCC(28)
70	-	-	562	540	41	11	3	1	βCCC(35)
71	-	-	515	495	12	3	3	1	βOCC(10)
72	-	409 (w)	448	430	4	1	1	0	τCCCC(33)+ωCCCC(14)
73	-	-	438	421	3	1	2	1	βCCC(11)+τOCCC(13)
74	-	-	417	400	0	0	3	1	βCOC(17)+βCCC(17)
75	-	298 (w)	354	341	1	0	7	2	βCCC(14)+β

									COC(25)
76	-	-	338	325	1	0	0	0	τHCOC(17)+τCCCC(43)
77	-	231(w)	278	267	1	0	3	1	βOCC(25)+βCCC(35)
78	-	-	230	221	1	0	2	1	βOCC(29)+βCOC(17)
79	-	-	206	198	1	0	1	0	τHCOC(49)
80	-	204 (w)	149	143	0	0	0	0	τHCCC(72)
81	-	161 (w)	120	115	0	0	1	0	βOCC(23)+βCCC(18)+ωCCCC(21)
82	-	146 (m)	72	69	0	0	2	1	τCCCC(30)
83	-	117 (m)	60	57	0	0	0	0	βCCC(27)+τCCCC(13)+ωCCCC(14)
84	-	85 (vs)	50	48	0	0	1	0	τCOCC(18)
85	-	-	33	32	1	0	2	1	τCOCC(52)+τCCCC(10)
86	-	-	28	27	0	0	1	0	τCCCC(37)+τOCCC(19)+τCOCC(11)
87	-	-	25	24	0	0	4	1	υOC(30)+υCC(15)+βCCC(12)

a scaling factor: 0.962 for B3LYP/6-311++G(d,p).
b Relative absorption intensities normalized with highest peak absorption equal to 100.
cRelative Raman intensities normalized to 100.
υ-stretching, β- in plane bending, ω- out plane bending, τ- torsion, vvw- very very weak, vw- very weak, w-weak, m-medium, s-strong, vs-very strong

O-H vibrations: The Oxygen-Hydrogen stretching vibrations are expected in the region 3300-3500 cm^{-1}. These bands are stronger and broader than those of the amine N–H stretches which appear in the same region. For the 3-furan-2-yl-4-phenyl-butyric acid. Observed at 3753 cm^{-1} by B3LYP/6-311++G (d,p) method. This pure mode shows 100% PED contribution.

C-H vibrations: The aromatic compounds and its derivatives show C-H stretching vibrations generally in the region above 3000 cm^{-1} for the benzene and less than 3000 cm^{-1} for non-aromatic compounds. In the experimental frequency, C-H stretching vibrations were observed at 3067 cm^{-1} to 2882 cm^{-1} in FT-Raman spectrum and 3180-2852 in the FT-IR spectra. The peak corresponding to C-H stretching vibration at the range 3170.-2918 cm^{-1} by theoretical method shows excellent agreement with experimental spectral values. The PED corresponding to this vibration contributes to 87-98%.

C-C vibrations: The aromatic ring modes are influenced more by C-C bands. The ring stretching vibrations (C-C) are expected within the region 1300-1000 cm^{-1}. In the present study, the bands which are of different intensities were observed at 1608, 1509, 1489, 1419, 1356, 1079 and 1037 cm^{-1} in FT-IR spectrum and Raman bands were identified at 1629, 1579, 1488, 1391, 1199 1127, 1078 and 1014 cm^{-1}. The theoretical values were obtained in the range of 1654-1012 cm^{-1} by B3LYP/6-311++G (d,p) method. It shows that the theoretical values are in good agreement with experimental data.

O-C Vibrations: The Oxygen-Carbon stretching modes generally exist in the region 1300-1000 cm^{-1}. The theoretical Oxygen-Carbon stretching vibrations were calculated at1050, 1030, 1015 and 739 cm^{-1}. Experimental bands observed at 1789, 1608 and 1037 cm^{-1} in FT-IR and at 1728, 1629 and 1014 cm^{-1} in FT Raman.

Molecular Electrostatic Potential (MEP)

The force acting on a proton located at a point through the electrical charge cloud generated through the molecules electrons and nuclei provides the Molecular Electrostatic Potential (MEP) at a given point p(x,y,z) in the vicinity of a molecule. Although the

molecular charge distribution remains unperturbed through the external test charge as no polarization occurs, the electrostatic potential of a molecule is a good tool in evaluating the reactivity of a molecule towards positively or negatively charged reactants. The MEP is characteristically pictured through mapping its values onto the surface reflecting the molecules boundaries. Electrostatic potential correlates with dipole moment, electro negativity and partial charges. Molecular electrostatic potential maps elucidate information about the charge distribution of a molecule, relative polarity and electrostatic potential properties of the nucleus and nature of electrostatic potential energy.

MEP is associated to the electronic density and is an expedient descriptor in understanding sites for electrophilic and nucleophilic reactions as well as hydrogen bonding interactions. MEP was calculated at the B3LYP/6-311++G (d,p) optimized geometry. A portion of a molecule that has a negative electrostatic potential is vulnerable to an electrophilic attack greater the negativity, the better. In MEP, maximum negative region represents the site for electrophilic attack indicated by red color while the maximum positive region represents nucleophilic attack indicated in blue color. While regions with the negative potential are over the electronegative Oxygen atom, the regions with the positive potential are over the hydrogen atoms. Potential increases in the order red<orange<yellow<green<blue Figure 5 provides a visual method to understand the relative polarity of the title molecule.

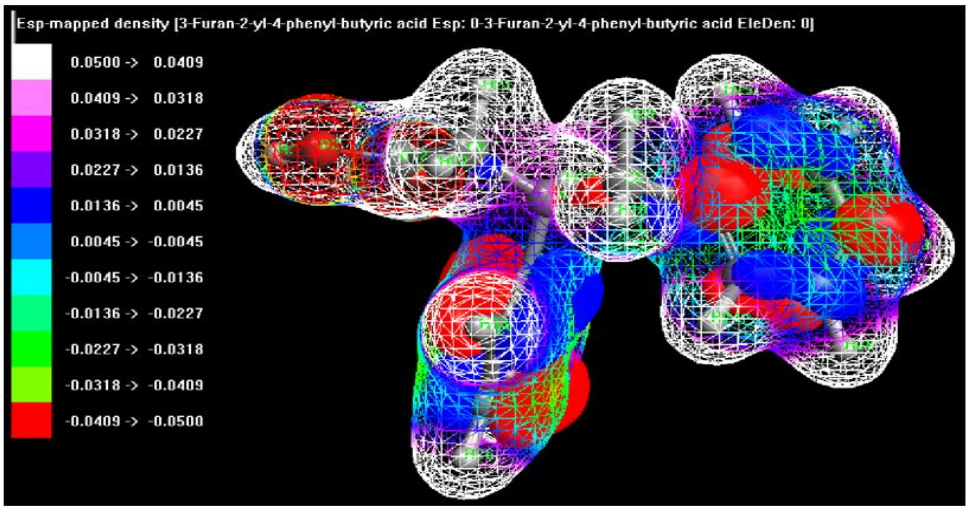

FIG.5. **Molecular Electrostatic Potential (MEP) of obtained by B3LYP/6-311++G(d,p) method.**

HOMO and LUMO analysis

The concept of HOMO and LUMO are of fundamental importance as it forms the basis of understating the chemical stability and reactivity of a given molecule. On the basis of chemical hardness, molecules can be classified as hard and soft molecules. Large HOMO-LUMO gap indicates that the title molecule is a hard molecule and minor HOMO-LUMO gap indicates that it is a soft molecule. The molecular stability and hardness are related inversely, *i.e*. the molecule with the least HOMO-LUMO gap is more reactive. The Ionization Potential (IP) is determined from the energy difference between the energy of the compound derived from electron transfer (E_{cation}-energy of radical cation) and the respective neutral compound (E_n) (Figure 6 and Table 4).

$$IP = E_{cation} - E_n;\ IP = -E_{HOMO}.$$

The Electron Affinity (EA) is computed from the energy difference between the neutral molecule (E_n) and the anion molecule (E_{anion})

$$EA = E_n - E_{anion};\ EA = -E_{LOMO}$$

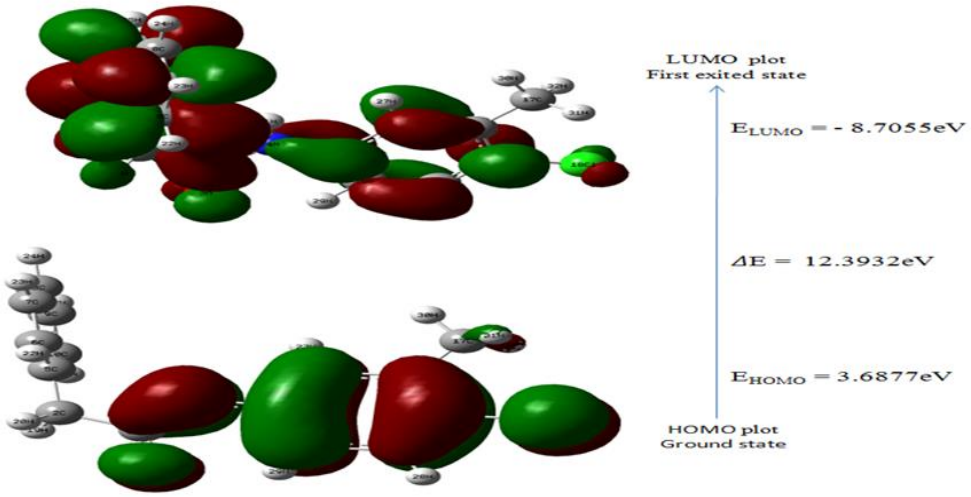

FIG.6**. Atomic orbital HOMO-LUMO composition of the frontier molecular orbital of 3-Furan-2-yl-4-Phenyl-Butyric Acid (2F4PBA).**

The minimum energy required to promote an electron is given by the energy difference between the orbitals (energy gap) and is therefore the most frequent and important energy transfer mechanism within a system. The orbitals provides information about the electron density which in turn is used in determining which part of the molecule is most actively participating in an energy transfer event.

The calculated quantum chemical parameters such as the Highest Occupied Molecular Orbital Energy (E_{HOMO}), the Lowest Unoccupied Molecular Orbital Energy (E_{LUMO}), energy gap (ΔE), Electronegativity (χ), chemical potential (μ), global hardness (η) and the softness (S) were calculated for the title molecule and tabulated in (Table 4). The concept of these parameters is related to each other, where

Chemical potential (μ) = ½ (E_{LUMO} +E_{HOMO}),

Electronegativity (χ) = $-\mu$ = - ½ (E_{LUMO} +E_{HOMO}),

Global hardness (η) = ½ (E_{LUMO} - E_{HOMO}),

Electrophilicity (ω) = μ^2 / 2η.

The inverse values of the global hardness are designated as the softness(S), it is given by S

Softness (S) = 1/η

TABLE 4**. Calculated energy values of the 3-Furan-2-yl-4-Phenyl-ButyricAcid (2F4PBA).**

Parameter	**Value**
E_{HOMO} (eV)	-8.70554
E_{LUMO} (eV)	3.6877
Ionization potential	8.705535
Electron affinity	-3.6877
Energy gap (eV)	12.39324
Electronegativity	2.508918
Chemical potential	-2.50892
Chemical hardness	6.196618
Chemical softness	0.080689
Electrophilicity index	0.507912

The calculated value of electrophilicity index=3.283 describes the biological activity of title compound. Also the bigger the dipole moment, the stronger will be the intermolecular interactions. Correlations have been deduced between electrophilicity of several chemical compounds and reaction rates in biochemical systems and such phenomena as allergic contact dermatitis. The energy of the HOMO and the ionization potential are related and describes the susceptibility of the molecule toward electrophilic attack. The energy of LUMO is directly linked to the electron affinity and illustrates the susceptibility of the molecule toward attack of nucleophiles. The energy gap between HOMO and LUMO indicates molecular chemical stability. The mesh diagrams of HOMO and LUMO are given in Figure 6. The positive and negative phase is represented in red and blue colour respectively.

Nonlinear Optical effects (NLO)

The electron correlation can change the value of hyperpolarisability which is very sensitive to the basis sets and level of theoretical approach employed. The polarizability α, the hyper polarizability β and the electric dipole moment μ of title compound are calculated by finite field method using B3LYP/6-311++G (d,p) polar=enonly basis set. In the presence of an applied electric field, the energy of a system is a function of the electric field. Polarizability and hyperpolarisability illustrate the response of a system in an applied electric field. This determines the Non Linear Optical properties (NLO) of the system. First hyper polarizability is a third rank tensor that can be defined by 3 x 3 x 3 matrix. The 27 components of the 3D matrix can be reduced to 10 components due to the Klein man symmetry. It can be given in the lower tetrahedral format. It is obvious that the lower part of the 3 x 3 x 3 matrixes is a tetrahedral (Table 5). The components of β are defined as the coefficients in the taylor series expansion of the energy in the external electric field. When the external electric field is weak and homogeneous, this expansion becomes:

$$E=E_0-\mu_\alpha F_\alpha-12\alpha_{\alpha\beta}F_\alpha F_\beta-16\beta_{\alpha\beta\gamma}F_\alpha F_\beta F_\gamma+\cdots$$

Where
E_0 is the energy of the unperturbed molecules
F_α is the field at the origin
μ_α is the component of dipole moment, is the component of polarizability
$\beta_{\alpha\beta\gamma}$is the component of first hyper polarizability.

TABLE 5. **The values of calculated dipole moment μ (D), polarizability (α) and first order hyperpolarisability (β) of 3-Furan-2-yl-4-Phenyl-ButyricAcid (2F4PBA).**

Title	Enter Values	Title	Enter Values	Title	Enter Values
βxxx	82.3961484	αxx	187.4973675	μx	1176805
βxxy	63.6182469	αxy	-5.4403967	μy	-0.3531568
βxyy	7.1028174	αyy	150.6268697	μz	0.56258
βyyy	-138.902403	αxz	-26.01046	μ(D)	1176805
βzxx	10.5813665	αyz	1.0303709		
βxyz	-29.5306966	αzz	151.94731		
βzyy	26.8952688	α (a.u)	163.3571824		
βxzz	55.4714412	α (e.s.u)	2.421×10^{-23}		
βyzz	-51.4569575	Δα (a.u)	326.7694605		
βzzz	44.6223981	Δα (e.s.u)	4.8427×10^{-23}		
βtot (a.u)	209.3322244				
βtot (e.s.u)	1.8085×10^{-30}				

The total static dipole moment μ, the mean polarizability α_0, the anisotropy of the polarizability Δα and the mean first hyperpolarisability β_0, using the x, y, z components are defined as:

$$\mu = (\mu_x^2+\mu_y^2+\mu_z^2)^{1/2}$$

$$\alpha_o = (\alpha_{xx}+\alpha_{yy}+\alpha_{zz})/3$$

$$\Delta\alpha = 2^{-1/2}[(\alpha^{xx}-\alpha^{yy})^2+(\alpha^{yy}-\alpha^{zz})^2+(\alpha^{zz}-\alpha^{xx})^2+6\alpha 2^{xx}]^{1/2}$$

$$\beta_0 = (\beta_x^2+\beta_y^2+\beta_z^2)^{1/2} \quad \text{where,}$$

$$= \beta_{xxx}+\beta_{xyy}+\beta_{xzz};$$

$$\beta_y = \beta_{yyy}+\beta_{yxx}+\beta_{yzz},$$

$$\beta_z = \beta_{zzz}+\beta_{zyy}+\beta_{zxx}.$$

The values of polarizability α, hyper polarizability β and the electric dipole moment μ are given in Table 5. Urea being one of the exemplary molecules used in the study of the NLO properties of the molecular systems. It is often used as a threshold value for comparative purposes. The computed values of μ, α and β for the title molecule are 0.876 D, 2.739 x 10^{-23} esu and 1.0579 x 10^{-30} esu respectively. The total molecular dipole moment of the title molecule from B3LYP/6-311++G (d,p) basis set is 0.886 D which is less than that of urea (μ(D)=1.373 D).The first order hyper polarizability of the title molecule is 5 times than that of urea (β_o= 0.373 x 10^{-30} esu). The B3LYP/6-311++G (d,p) calculated energy gap is E=12.3932eV which is lower than urea (ΔE=6.706 eV). These results indicate that the title compound may be a good candidate of NLO material and can also be considered to be an important class of compound in medical chemistry because if its high electrophilicity index (0.50791).

Mulliken charge distribution and Fukui function

The Mulliken Population Analysis (MPA) is calculated using the Natural Population Analysis of the title molecule (NPA) with B3LYP 6-311++G (d,p) method. The charge and multiplicity are varied in order to compare the variation in the Mulliken charges in each case.

Distribution of positive and negative charges is the important to increasing or decreasing of bond length between the atoms. In the present study, the optimized molecular geometry was employed in single-point energy calculations. The DFT calculations for the anions and cations were done using the ground state with double multiplicity. The individual atomic charges, calculated by MPA have been used to calculate the Fukui functions in Table 6 shows the f_k and $(sf)_k$ values for the compound, using which one can find the complexities associated with f_k values due to the negative values being removed in the $(sf)_k$ values.

The calculated Mulliken charge values of the title molecule are listed in Table 6. It can be observed graphically in Figure 7 that the carbon atom C-9 has most positive charge of 0.3910, 0.3870 where the charge and multiplicity are (0,1), (-1,2) and (1,2) respectively. The least positive value is that of H-26 is 0.1120. Similarly the maximum negative charge is that of the carbon atom C-17 with a value of -0.0600, -0.0700 and 0.0230. The least negative value is that of C-7 which is -0.6860.Three oxygen atoms have negative charges and all the hydrogen atoms have positive charges. The result suggests that the oxygen atoms acts as lone pair donor and the charge transfer takes place from O to C due to electron accepting substitutions at that position in the title molecule.

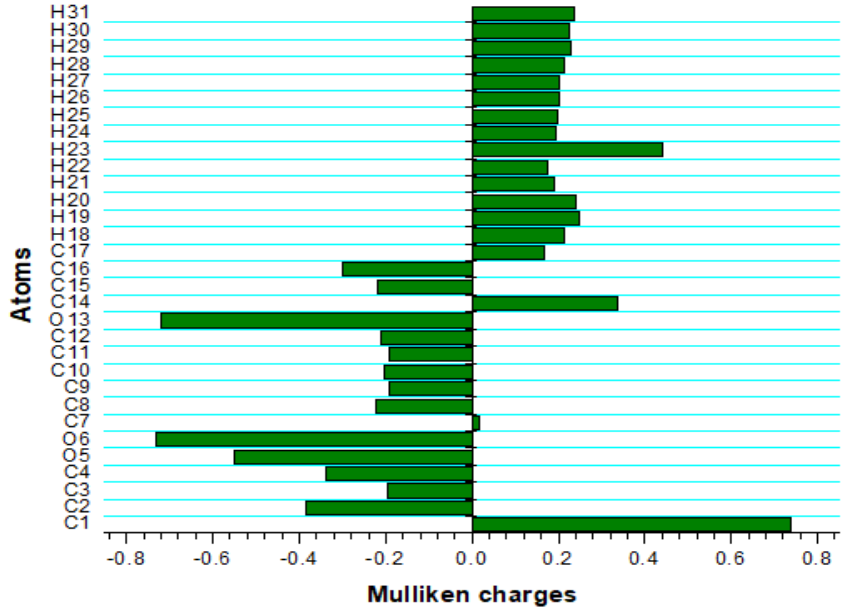

FIG.7. **The histogram of calculated Mulliken charges of 3-furan-2-yl-4-phenyl-butyric acid.**

The electron density based local reactivity descriptors such as Fukui functions are proposed to clarify the chemical selectivity or reactivity at a particular site of a chemical system. Electron density is a property that contains all the evidence about the molecular system and plays an important role in calculating nearly all the chemical quantities proposed a finite difference approach to compute Fukui function indices *i.e.* nucleophilic, electrophilic and radical attacks (Table 6).

TABLE 6. **Mulliken charge distribution, Fukui function and local softness corresponding to (0,1), (-1,2) and (1,2) charge and multiplicity of- 3-furan-2-yl-4-phenyl-butyric acid (2F4PBA).**

Atom	**Mulliken atomic charges**			**Fukui functions**			**Local softness**		
	0,1 (N)	**N +1 (-1, 2)**	**N-1 (1,2)**	**fr_+**	**fr_-**	**fr_0**	**sr_+fr_+**	**sr_-fr_-**	**$sr_0\ fr_0$**
C_1	-0.2020	-0.2460	-0.1860	-0.0440	-0.0160	-0.0300	-0.0090	-0.0030	-0.0060
C_2	-0.2810	0.4610	-0.2670	0.7420	-0.0140	0.3640	0.1550	-0.0090	0.0760
C_3	-0.1470	-0.1090	-0.1230	0.0380	-0.0240	0.0070	0.0080	-0.0050	0.0010
C_4	0.1340	-0.1600	0.1500	-0.2940	-0.0160	-0.1550	-0.0610	-0.0030	-0.0320
O_5	-0.4590	-0.4570	-0.4360	0.0020	-0.0230	-0.0110	0.0000	-0.0050	-0.0020
O_6	0.6710	0.8320	0.5910	0.1610	0.0800	0.1200	0.0330	0.0170	0.0250
C_7	-0.6860	-0.4600	-0.6340	0.2260	-0.0520	0.0870	0.0470	-0.0110	0.0180
C_8	-0.4310	-0.3940	-0.3510	0.0370	-0.0800	-0.0220	0.0080	-0.0170	-0.0050
C_9	0.3910	0.4660	0.3930	0.0750	-0.0010	0.0370	0.0160	0.0000	0.0080
C_{10}	-0.4040	-0.4010	-0.3630	0.0030	-0.0420	-0.0190	0.0010	-0.0090	-0.0040
C_{11}	-0.1140	-0.1270	-0.0580	-0.0130	-0.0560	-0.0350	-0.0030	-0.0120	-0.0070
C_{12}	-0.2810	-0.2640	-0.2960	0.0170	0.0150	0.0160	0.0040	0.0030	0.0030
O_{13}	-0.0370	-0.1300	0.0160	-0.0940	-0.0520	-0.0730	-0.0200	-0.0110	-0.0150
C_{14}	-0.3840	-0.3690	-0.3710	0.0150	-0.0130	0.0010	0.0030	-0.0030	0.0000
C_{15}	-0.4600	-0.4650	-0.3590	-0.0050	-0.1010	-0.0530	-0.0010	-0.0210	-0.0110

C_{16}	0.3870	0.3710	0.3800	-0.0160	0.0070	-0.0050	-0.0030	0.0010	-0.0010
C_{17}	-0.0600	-0.0700	-0.0230	-0.0100	-0.0360	-0.0230	-0.0020	-0.0080	-0.0050
H_{18}	0.2740	-0.2040	0.2870	-0.4780	-0.0120	-0.2450	-0.1000	-0.0030	-0.0510
H_{19}	0.2060	-0.4850	0.2380	-0.6900	-0.0320	-0.3610	-0.1440	-0.0070	-0.0760
H_{20}	0.1370	0.0900	0.1410	-0.0470	-0.0040	-0.0250	-0.0100	-0.0010	-0.0050
H_{21}	0.1840	0.1200	0.1920	-0.0640	-0.0080	-0.0360	-0.0130	-0.0020	-0.0080
H_{22}	0.1870	-0.0290	0.2220	-0.2150	-0.0360	-0.1250	-0.0450	-0.0070	-0.0260
H_{23}	0.1440	0.1400	0.2040	-0.0030	-0.0600	-0.0320	-0.0010	-0.0130	-0.0070
H_{24}	0.2140	0.1570	0.2700	-0.0560	-0.0560	-0.0560	-0.0120	-0.0120	-0.0120
H_{25}	0.1490	0.1030	0.1990	-0.0460	-0.0500	-0.0480	-0.0100	-0.0100	-0.0100
H_{26}	0.1120	0.1120	0.1320	0.0000	-0.0200	-0.0100	0.0000	-0.0040	-0.0020
H_{27}	0.1370	0.1230	0.1660	-0.0140	-0.0280	-0.0210	-0.0030	-0.0060	-0.0040
H_{28}	0.1460	0.0890	0.2120	-0.0570	-0.0660	-0.0610	-0.0120	-0.0140	-0.0130
H_{29}	0.1770	0.1360	0.2470	-0.0420	-0.0690	-0.0550	-0.0090	-0.0140	-0.0120
H_{30}	0.1310	0.0780	0.2030	-0.0530	-0.0720	-0.0630	-0.0110	-0.0150	-0.0130
H_{31}	0.1660	0.0910	0.2250	-0.0750	-0.0600	-0.0670	-0.0160	-0.0120	-0.0140

Fukui indices are reactivity indices that provide information about which atoms in a molecule have a greater tendency to either loose or accept an electron. This information plays a vital role in helping the chemists to interpret which atoms are more prone to undergoing a nucleophilic or an electrophilic attack. The functions are defined as

$$F(r) = \frac{\delta \rho(r)}{\partial N}_{\underset{\sim}{r}}$$

Where
$\rho(r)$ is the electronic density
N is the number of electrons and r is the external potential exerted by the nucleus.

The Fukui function is a local reactivity descriptor that indicates the ideal regions where a chemical species will change its density with the modification in the number of electrons. Therefore, it indicates the tendency of the electronic density to deform at a given position upon accepting or donating electrons also, it is possible to define the corresponding condensed or aromatic Fukui functions on the k^{th} atom site as,

$f_k^+ = q_k (N+1) - q_k (N)$; for nucleophilic attack,
$f_k^- = q_k (N) - q_k (N-1)$; for electrophilic attack,
$f_k^0 = ½ (q_k (N+1) - q_k (N-1)$; for radical attack.

Where +, -, 0 signs show nucleophilic, electrophilic and radical attack respectively.

In these equations, q_k is the atomic charge at k^{th} atomic site for the Neutral (N), anionic (N+1) and cationic (N-1) chemical species. The Fukui function allows analyzing the distribution of the active sites in a molecule for which the value of the function is totally dependent on the type of charges used. To solve the negative Fukui function problem, different attempts have been made by various groups introduced the atomic descriptor to determine the local reactive sites of the molecular system.

Thermodynamic properties

The partition function is one of important parameters of thermodynamics (Figure 8). The partition function associates thermodynamics, spectroscopy and quantum theory. The partition functions are further classified as (i) translational partition function, (ii) rotational partition function, (iii) vibrational partition function and (iv) electronic partition function. The standard

statistical thermodynamic functions such as standard heat capacity (C_P), standard entropy (S) and standard enthalpy changes (H) were obtained from the theoretical harmonic frequencies on the basis of vibrational analysis at B3LYP/6-311++G (d,p) level using thermo.pl software and listed in Table 7. From the observations in the above Table 6, all the values of C_p, S and H increase with the increase in temperature from 100 K to 1000 K. This is accredited to the enhancement of the molecular vibration. The temperature increases because at a constant pressure, the values of Cp, S and H are equal to the quantity of temperature. The relations between these thermodynamic properties and temperatures are fitted by quadratic equations and the corresponding fitting factor (R_2). It was found to be 0.99999, 0.9997 and 0.9994 for entropy, heat capacity, and enthalpy, respectively. The temperature dependence correlation graph is represented in Figure 8 and the corresponding fitting equations are shown below:

$S=275.86486+0.96322T-1.91631 \times 10^{-4} T^2$ ($R^2=0.9999$).
$C_P=5.91321+0.94689T-3.77084 \times 10^{-4} T^2$ ($R^2=0.9997$).
$H=-8.62969+0.09844T+2.70257 \times 10^{-4} T^2$ ($R^2=0.9994$)

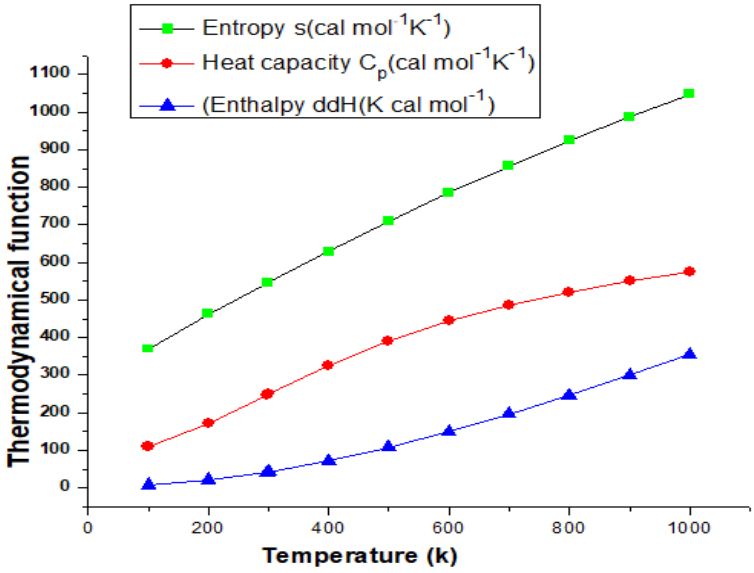

FIG.8. **Graphs representing dependence of entropy, specific heat capacity and enthalpy on temperature of -3-furan-2-yl-4-phenyl-butyric acid (2F4PBA).**

TABLE 7. **Thermodynamics functions of - 3-furan-2-yl-4-phenyl-butyric acid with different temperature.**

T (K)	S (J/mol.K)	Cp (J/mol.K)	ddH (kJ/mol)
100	369.748	109.683	7.861
200	463.247	170.615	21.695
298.15	545.33	247.041	42.123
300	546.863	248.529	42.581
400	629.13	325.693	71.363
500	709.101	391.305	107.323
600	785.299	444.208	149.197
700	857.084	486.744	195.82
800	924.42	521.452	246.286
900	987.551	550.245	299.914
1000	1046.814	574.452	356.182

The thermodynamic data provides the required data for the further study on the title molecule. Thermodynamic energies according to the relationships of thermodynamic functions and estimate directions of chemical reactions in accordance to the second law of thermodynamics in thermochemical field.

Molecular docking study

Auto Dock suite 1.5.6 (ADT) is graphical front end for running auto dock automated docking software designed to predict how small molecules (substrates or drug candidates) bind to a receptor of known 3D structure. The title compound was selected to be docked into the active site of the protein 4Y95 which belongs to the class of proteins exhibiting the property as a (BTK) Bruton's Tyrosine Kinase expression inhibitor Ibrutinib (PCI-32765) in B-Cell Acute Lymphoblastic Leukemia (B-ALL). Bruton's Tyrosine Kinase (BTK) Bruton's Tyrosine Kinase (BTK) is a cytoplasmic, non-receptor tyrosine kinase which is expressed in most of the hematopoietic cells and plays an important role in many cellular signaling pathways. B cell malignancies are dependent on BCR signaling, thus making BTK an efficient therapeutic target. The transcription factor BTK plays a significant role in cellular response to systemic oxygen levels in mammals (Figure 9). BTK activity is controlled by a host of post translational modifications: hydroxylation, acetylation and phosphorylation. When a body suffers with hypoxia a region of the body is deprived of adequate oxygen supply at the tissue level leading to stiffness. The ligand was docked into the functional sites of the selected protein and minimum docking energy value was examined. Auto dock results designate the binding position and bound conformation of the peptide, together with an approximation of its interaction. Docked conformation which had the lowest binding energy was chosen to study the mode of binding. The molecular docking binding energies (kcal/mol) and inhibition constants (mm) were also obtained and listed in Table 8. The 3-Furan-2-yl-4-Phenyl-Butyric Acid (2F4PBA) ligand interactions with protein 4Y95 is shown in Figure 9. A minimum binding energy of -4.79 kcal/mol was seen in the interaction.

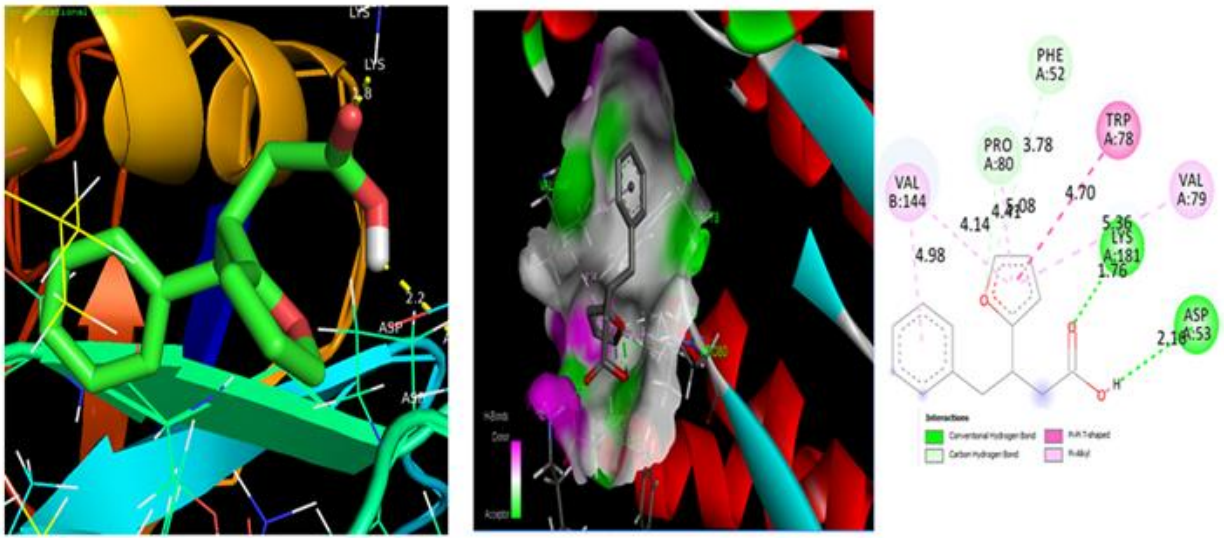

FIG.9 (a). **Docking and Hydrogen bond interactions of - 3-furan-2-yl-4-phenyl-butyric acid (2F4PBA) with 4Y9Z protein;** (b). **Docking and Hydrogen bond interactions of - 3-furan-2-yl-4-phenyl-butyric acid (2F4PBA) with 4Y9Z protein.**

TABLE 8. **Hydrogen bonding and molecular docking with 4Y95, BTC expression inhibitor protein targets.**

Protein (PDB ID)	Bonded residues	Bond distance (Å)	Inhibition constant (µmol)	Binding energy (kcal/mol)	Intermolecular energy (kcal/mol)	Reference RMSD (Å)
4Y95	ASP	2.1	310.06	-4.79	-6.58	110.68
	LYS	1.76				

Conclusion

The complete vibrational spectral analysis and DFT theoretical calculation were performed for title molecule. The optimized geometric parameters (bond lengths and bond angles) are theoretically determined and compared with the structurally similar

molecules. The interaction energy, related to resonance in the molecule, is electron withdrawing from the ring through π^*(C7-C8) of the NBO conjugated with π^*(C9-C16) resulting with large stabilization energy of 263.92 kJ/mol. The large difference in HOMO and LUMO energy supports the charge transfer model of interaction within the molecule. Finally, the theoretical results showed an acceptable general agreement with the experimental record. The predicted MEP figure revealed the negative and positive regions of the molecule. The computed values of μ, α and β for the title molecule are 0.876 D, 2.739 x 10^{-23} esu and 1.0579 x 10^{-30} esu respectively. The first order hyper polarizability of the title molecule is 3 times than that of urea (βo= 0.3728 x 10^{-30} esu) and the calculated energy gap is E= 12.3932eV which is lower than urea (ΔE= 6.7063 eV). These results indicate that the title compound is a good candidate of NLO material and can also be considered to be an important class of compound in medical chemistry because if its high electrophilicity index (0.5079). The FT-IR and FT-Raman spectra of the title molecule are observed with the experimental and calculated vibrational wavenumbers and their PED is noted. Thermodynamic properties in the range from 100 to 1000 K are obtained. The gradients of C_p, S and H increases, as the temperature increases which is attributed to the enhancement of the molecular vibration. The charge and multiplicity are varied in order to compare the variation in the Mullikan charges in each case. The electron density based local reactivity descriptors such as Fukui functions are proposed. The title compound was selected to be docked into the active site of the protein 4Y95 which belongs to the class of proteins exhibiting the property as a Bruton's Tyrosine Kinase (BTK) expression inhibitor.

References

1. Vueba ML, Pina ME, Veiga F, et al. Conformational study of ketoprofen by combined DFT calculations and Raman spectroscopy. Int J Pharma. 2006;307(1):56-65.
2. Musa KA, Eriksson LA. Photo degradation mechanism of non-steroidal anti-inflammatory drugs containing thiophene moieties: Suprofen and Tiaprofenic acid. J Phys Chem B. 2009;113(32):11306-11313.
3. Ottou Abe MT, Correia NT, Ndjaka JM, et al. A comparative study of ibuprofen and ketoprofen glass forming liquids by molecular dynamics simulations. J Chem Phys. 2015;143(16):164506.
4. Hess Jr BA, Schaad LJ, Carsky P, et al. Ab initio calculations of vibrational spectra and their use in the identification of unusual molecules. Chem Rev. 1986;86(4):709-730.
5. Becke AD. A new mixing of Hartree–Fock and local density-functional theories. J Chem phys. 1993;98(2):1372-1377.
6. Lee C, Yang W, Parr RG, et al. Development of the Colle Salvetti correlation energy formula into a functional of the electron density. Phys Rev B. 1988;37(2):785.
7. Li XH, Zhang RZ, Zhang XZ, et al. Natural bond orbital analysis of some para substituted N-nitrosoacetanilide biological molecules. Struct Chem. 2009;20(6):1049-1054.
8. Chocholoušová J, Špirko V, Hobza P, et al. First local minimum of the formic acid dimer exhibits simultaneously red-shifted O–H···O and improper blue-shifted C–H···O hydrogen bonds. Phys Chem. 2004;6(1):37-41.
9. Reed AE, Curtiss LA, Weinhold F, et al. Intermolecular interactions from a natural bond orbital, donor acceptor viewpoint. Chem Rev. 1988;88(6):899-926.
10. Muthu S, Ramachandran G, Paulraj EI, et al. Quantum mechanical study of the structure and spectroscopic (FTIR, FT-Raman), first-order hyperpolarisability and NBO analysis of 1, 2-benzoxazol-3-ylmenthane sulfonamide. Spectrochim Acta A Mol and Biomol Spectrosc. 2014;128:603-613.
11. Weinhold F, Landis CR. Valency and bonding: a natural bond orbital donor acceptor perspective. Cambridge University Press.2005.
12. Sıdır İ, Sıdır YG, Kumalar M, et al. Ab initio Hartree–Fock and density functional theory investigations on the conformational stability, molecular structure and vibrational spectra of 7-acetoxy-6-(2, 3-dibromopropyl)-4, 8-dimethylcoumarin molecule. J Mol Struct. 2010;964(1-3):134-151.
13. Parr RG, Pearson RG. Absolute hardness: companion parameter to absolute electronegativity. J Am Chem Soc. 1983;105(26):7512-7516.
14. Mulliken RS. Electronic population analysis on LCAO–MO molecular wave functions. I. J Chem Phys. 1955; 23(10):1833-1840.
15. Henriksson J, Saue T, Norman P, et al. Quadratic response functions in the relativistic four-component Kohn-Sham approximation. J Chem Phys. 2008;128(2):024105.

16. Parr RG, Yang W. Density functional approach to the frontier electron theory of chemical reactivity. J Am Chem Soc. 1984;106(14):4049-4050.
17. Yang W, Parr RG. Hardness, softness and the Fukui function in the electronic theory of metals and catalysis. Proc o Natl Acad Sci. 1985;82(20):6723-6726.
18. Henriksson J, Saue T, Norman P, et al. Quadratic response functions in the relativistic four-component Kohn-Sham approximation. J Chem Phys. 2008;128(2):024105.
19. Parr RG, Chattaraj PK. Principle of maximum hardness. J Am Chem Soc. 199;113(5):1854-1855.
20. Parr RG, Pearson RG. Absolute hardness: companion parameter to absolute electronegativity. J Am Chem Soc. 1983;105(26):7512-7516.